

PLANT SCIENCE

Loss of *AvrSr50* by somatic exchange in stem rust leads to virulence for *Sr50* resistance in wheat

Jiapeng Chen,^{1,2,3*} Narayana M. Upadhyaya,^{2*} Diana Ortiz,^{2*} Jana Sperschneider,⁴ Feng Li,⁵ Clement Bouton,⁶ Susan Breen,² Chongmei Dong,¹ Bo Xu,² Xiaoxiao Zhang,² Rohit Mago,² Kim Newell,² Xiaodi Xia,² Maud Bernoux,² Jennifer M. Taylor,² Brian Steffenson,⁵ Yue Jin,^{5,7} Peng Zhang,¹ Kostya Kanyuka,⁶ Melania Figueroa,⁵ Jeffrey G. Ellis,² Robert F. Park,^{1†} Peter N. Dodds^{2†}

Race-specific resistance genes protect the global wheat crop from stem rust disease caused by *Puccinia graminis* f. sp. *tritici* (*Pgt*) but are often overcome owing to evolution of new virulent races of the pathogen. To understand virulence evolution in *Pgt*, we identified the protein ligand (*AvrSr50*) recognized by the *Sr50* resistance protein. A spontaneous mutant of *Pgt* virulent to *Sr50* contained a 2.5 mega-base pair loss-of-heterozygosity event. A haustorial secreted protein from this region triggers *Sr50*-dependent defense responses in planta and interacts directly with the *Sr50* protein. Virulence alleles of *AvrSr50* have arisen through DNA insertion and sequence divergence, and our data provide molecular evidence that in addition to sexual recombination, somatic exchange can play a role in the emergence of new virulence traits in *Pgt*.

Wheat is a staple crop that contributes 20% of human calorific intake, but its production is affected by pathogens, including the fungus *Puccinia graminis* f. sp. *tritici* (*Pgt*), which causes stem rust disease (1, 2). Deployment of disease-resistance genes through breeding provides cost-effective control of wheat rust diseases (3). Race-specific resistance is generally conferred by immune receptors of the nucleotide-binding leucine-rich repeat (NLR) class, which recognize pathogen effector proteins delivered into the host cell during infection, often known as avirulence (*Avr*) proteins (4). However, pathogen evolution to overcome resistance is a common occurrence and necessitates continued efforts to identify new resistance gene sources. The emergence of virulent races of *Pgt* in East Africa, particularly the Ug99 race group, has posed a threat to global wheat production (2, 5).

A number of NLR-encoding rust resistance genes have been isolated from wheat (6). Here, we identify an *Avr* protein recognized by one of these receptors.

The *Sr50* resistance gene encodes an NLR protein and provides resistance against all race groups of *Pgt* worldwide, including Ug99 (7). To identify the corresponding *AvrSr50* gene, we generated next-generation sequence (NGS) data from *Pgt* isolate *Pgt279* and a spontaneous mutant derived from this isolate with virulence to *Sr50*, *Pgt632* (fig. S1) (7). Because the wheat-infecting uredinial stage of *Pgt* has a dikaryotic (n+n) genome with two haploid nuclei (8), *Pgt279* is likely heterozygous for *AvrSr50*, with the virulent derivative *Pgt632* resulting from mutation of the dominant avirulence allele. We identified ~1.1 million heterozygous variants [single/multiple nucleotide variants (SNVs/MNVs) and small insertions

and deletions; ~1% of sites] in each isolate compared with the reference genome PGTAus-pan (9, 10). Because known *Avr* genes from the model flax rust fungus *Melampsora lini* encode secreted proteins expressed in haustoria—specialized structures that penetrate the host cell (11, 12)—we examined the 592 haustorial secreted protein (HSP) genes annotated in *Pgt* (9) for mutations. Although no new nonsynonymous variants were identified, 18 HSP genes showed loss-of-heterozygosity in *Pgt632* (tables S1 and S2 and fig. S2). Mapping heterozygosity rates in *Pgt632* and *Pgt279* for each contig in the genome assembly revealed loss-of-heterozygosity in a region of at least 2.5 Mbp spanning four full scaffolds and part of a fifth (Fig. 1A, fig. S3, and table S3).

Loss of heterozygosity in *Pgt632* could result from deletion, which would halve the DNA copy number per dikaryotic genome of the affected region, or by somatic exchange between the two haplotypes, which would retain the DNA copy number. The normalized depth of sequencing read coverage for contigs in the loss-of-heterozygosity region was similar to the remainder of the genome in both *Pgt632* and *Pgt279* (table S4), suggesting no loss of DNA copy number. Likewise, there were no significant differences in coverage depth for individual gene loci between the isolates or genome regions (fig. S4, A to C), with a uniform read depth ratio between *Pgt279* and *Pgt632* close to 1 (Fig. 1B). Thus, we conclude that

¹Plant Breeding Institute, School of Life and Environmental Sciences, University of Sydney, Cobby, NSW, Australia. ²Commonwealth Scientific and Industrial Research Organisation, Agriculture and Food, Canberra, ACT, Australia. ³Judith and David Coffey Life Lab, Charles Perkins Centre, University of Sydney. ⁴Centre for Environment and Life Sciences, Commonwealth Scientific and Industrial Research Organisation, Agriculture and Food, Perth, WA, Australia. ⁵Department of Plant Pathology and The Stakman-Borlaug Center for Sustainable Plant Health, University of Minnesota, St. Paul, MN, USA. ⁶Biointeractions and Crop Protection, Rothamsted Research, Harpenden, AL5 2JQ, UK. ⁷United States Department of Agriculture—Agricultural Research Service (USDA-ARS), Cereal Disease Laboratory, St. Paul, MN, USA. ^{*}These authors contributed equally to this work. [†]Corresponding author. Email: robert.park@sydney.edu.au (R.F.P.); peter.dodds@csiro.au (P.N.D.)

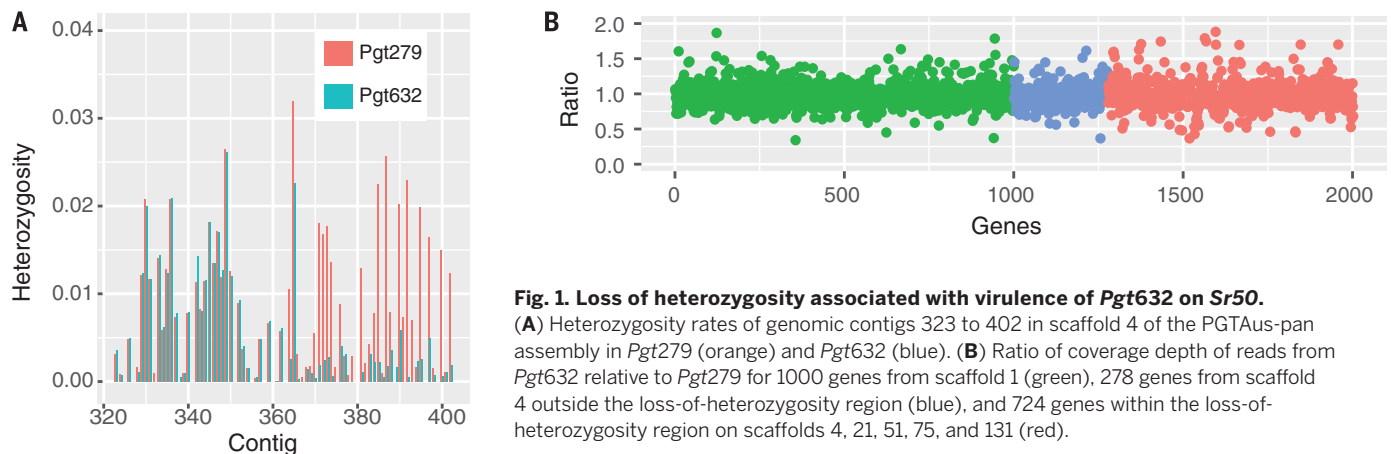


Fig. 1. Loss of heterozygosity associated with virulence of *Pgt632* on *Sr50*.

(A) Heterozygosity rates of genomic contigs 323 to 402 in scaffold 4 of the PGTAus-pan assembly in *Pgt279* (orange) and *Pgt632* (blue). (B) Ratio of coverage depth of reads from *Pgt632* relative to *Pgt279* for 1000 genes from scaffold 1 (green), 278 genes from scaffold 4 outside the loss-of-heterozygosity region (blue), and 724 genes within the loss-of-heterozygosity region on scaffolds 4, 21, 51, 75, and 131 (red).

the loss of one haplotype in this region of the *Pgt632* genome has been accompanied by duplication of the other haplotype. This was supported by quantitative polymerase chain reaction determination of relative copy number for shared

and haplotype-specific sequences (fig. S4, D and E). Although it is not clear how genetic exchange occurs between the two separate haploid nuclei, which are thought to replicate independently (13), genetic evidence suggests that nuclear exchange

and recombination between coinoculated rust isolates can result in previously unknown virulence combinations (14, 15). There is also evidence for nuclear fusion in *Pgt* (16), and somatic hybridization has been postulated as a mechanism underlying the emergence of new lineages in asexual rust populations (17–19).

The loss-of-heterozygosity region in *Pgt632* contains 24 annotated HSP genes in the reference genome assembly, and the allelic variants of these genes missing from *Pgt632* but present in *Pgt279* are candidates to encode *AvrSr50*. Of these genes, 21 showed two allelic types in *Pgt279* with SNV frequencies close to 0.5 (fig. S5), and only a single sequence variant in *Pgt632*. The two allele sequences of these genes were extracted from the NGS data (table S5), and the *Pgt279*-specific allele was used to generate in planta expression constructs. Another three HSP genes are part of multigene families, and sequences representing these genes were obtained with DNA amplification, with all 20 variants retained for functional screening because it was not possible to assign them to haplotypes. In total, 41 different HSP proteins (table S6) were expressed in *Nicotiana benthamiana* as cytosolic proteins lacking their signal peptides along with the Sr50 resistance protein. A single *AvrSr50* candidate, HSP#8 (HSGS210|asmb1_13131|m.9539), triggered a cell death response when coexpressed with *Sr50* (Fig. 2A and fig. S6). Coexpression with the related Sr33 resistance protein produced no response (Fig. 2A and fig. S7A), confirming the specificity of this recognition event, which was also observed in *Nicotiana tabacum* (Fig. 2B). A recombinant *Barley stripe mosaic virus* (20) expressing the *AvrSr50* candidate was unable to infect wheat plants containing *Sr50* (Fig. 2C) but retained virulence on susceptible wheat, confirming *AvrSr50* recognition by *Sr50* in wheat and showing that the *Sr50*-resistance response is effective against virus infection. The *AvrSr50* protein interacted with the Sr50 protein, but not with Sr33, in a yeast-two-hybrid assay (Fig. 2D and fig. S7B). The 132-amino acid *AvrSr50* protein has no homology to known proteins detected by either sequence or structure modeling searches, including in related *Puccinia* species.

A discontinuity in mapping of *Pgt632* NGS reads to the reference genome *AvrSr50* sequence suggested that the alternative (virulence) allele of *AvrSr50* is disrupted by a DNA insertion. De novo assembly of *Pgt632* sequencing reads resulted in two separate contigs containing the 5' and 3' regions of *AvrSr50*, each fused to an unrelated sequence, and the presence of this insertion was confirmed by means of DNA amplification (figs. S8 and S9 and data file S1). Examination of NGS data for genomes of other Australian *Pgt* isolates avirulent on *Sr50* (9) showed that 21-0, 326-1,2,3,5,6, and 194-1,2,3,5,6 were each heterozygous for the same two allelic variants of *AvrSr50* as in *Pgt279*, whereas rust strain 126-5,6,7,11 contained two alleles with identical coding sequence to the avirulence allele of *AvrSr50* but distinguished by SNVs in the 5' and 3' regions (fig. S10). Sequencing of RNA from wheat infected with these

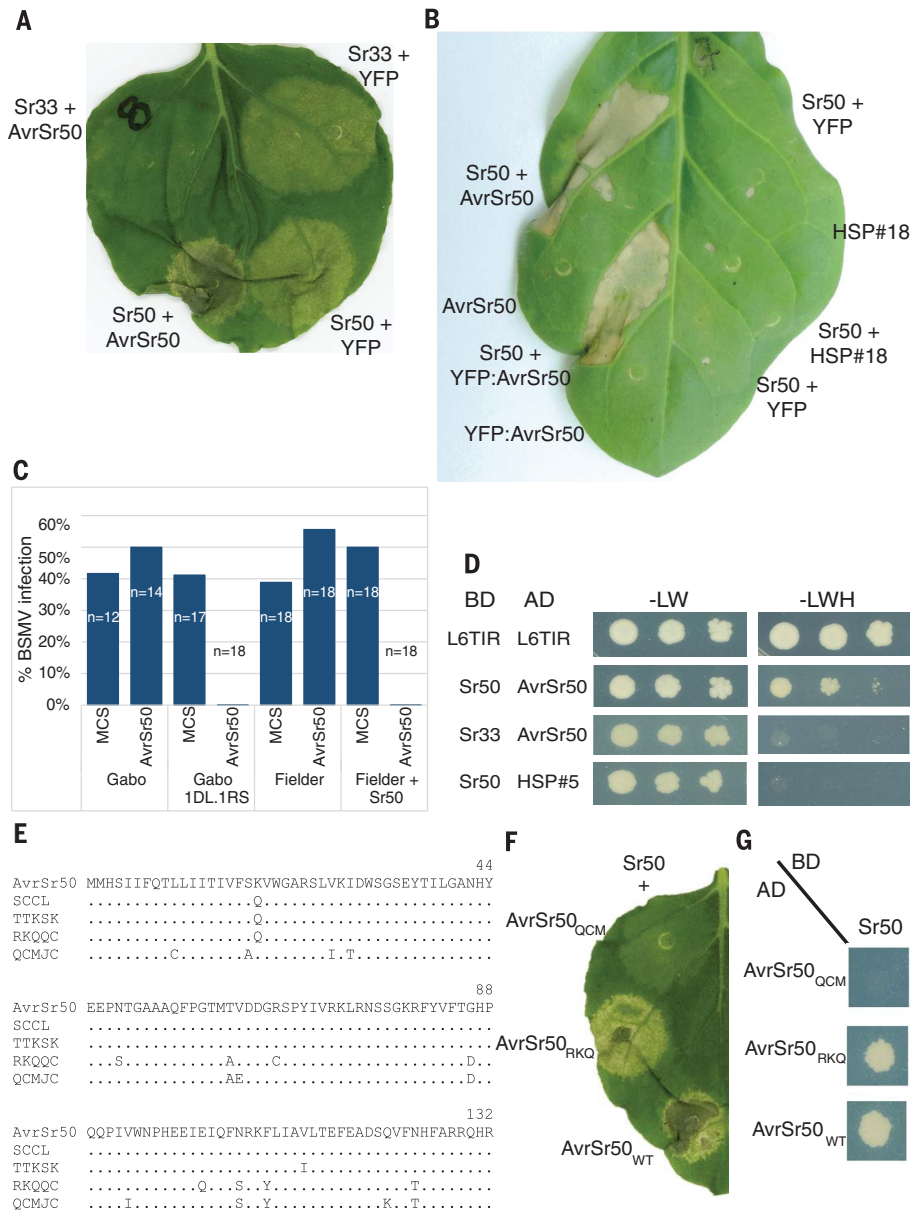


Fig. 2. The *AvrSr50* effector is recognized by *Sr50*. (A) Transient expression in *N. benthamiana* of Sr50:HA or Sr33:HA with YFP:AvrSr50 or YFP alone. HA, hemagglutinin; YFP, yellow fluorescent protein. Images were taken 4 days after infiltration. (B) Transient coexpression in *N. tabacum* of Sr50:HA with AvrSr50, YFP:AvrSr50, HSP#18, or YFP alone. Images taken 2 days after infiltration. (C) Infection of wheat lines Gabo, Gabo-1DL.1RS (contains *Sr50*), Fielder, and transgenic Fielder expressing *Sr50* with the *Barley stripe mosaic virus* expression vector containing either *AvrSr50* or a noncoding multiple cloning site (MCS). (D) Growth of yeast strains coexpressing Sr50 or Sr33 fused to the GAL4 DNA binding domain (BD) with *AvrSr50* or HSP#5 fused to the GAL4 activation domain (AD) on control media lacking leucine and tryptophan (-LW) or selective media additionally lacking histidine (-LWH). Self-interaction of the flax L6 protein TIR domain is a positive control (26). A 10-fold dilution series is shown. (E) Amino acid sequence of *AvrSr50* and variants found in *Pgt* isolates of races SCCL, TTKSK, RKQQC, and QCMJC. (F) Transient expression in *N. benthamiana* of Sr50:HA with YFP-tagged *AvrSr50* wild type (WT) and variant alleles from races RKQQC and QCMJC. Image was taken 4 days after infiltration. (G) Growth of yeast strains coexpressing BD:Sr50 with *AvrSr50* wildtype, RKQQC, and QCMJC variants on selective media.

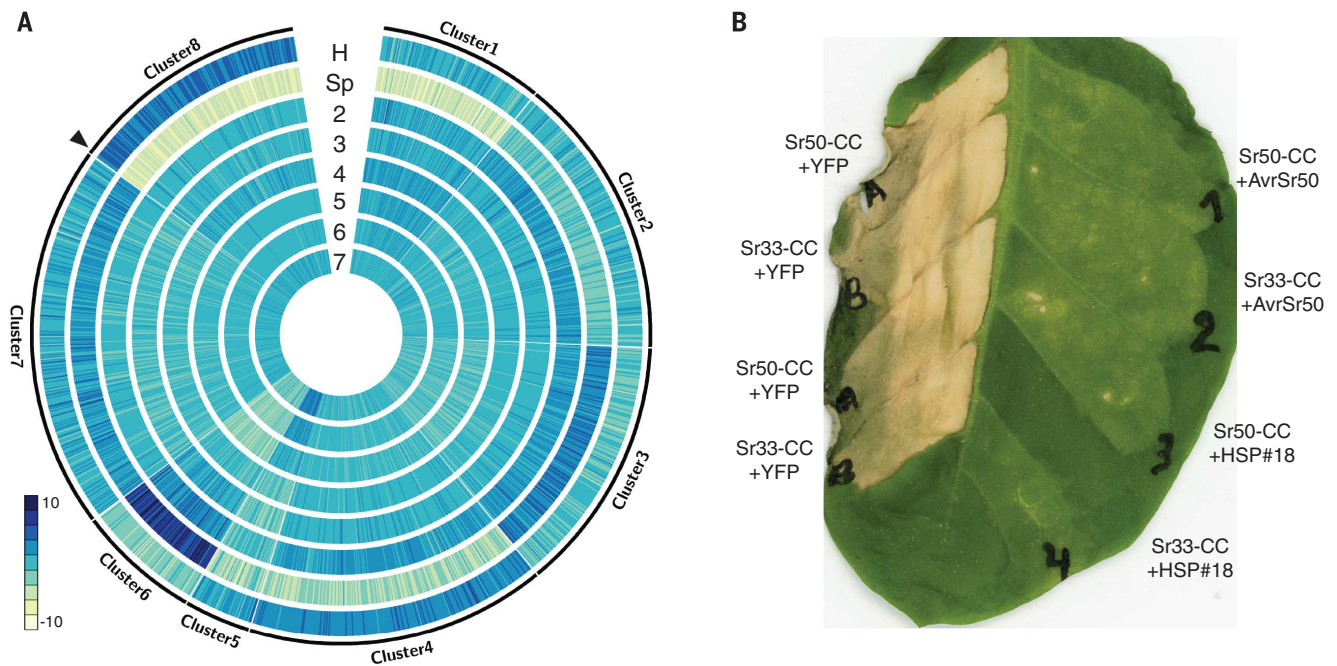


Fig. 3. *AvrSr50* is expressed early in infection and can suppress cell death responses. (A) Clustering analysis of *Pgt* secretome expression profiles. Blue color intensity indicates relative expression levels (relative *rlog* transformed counts) in haustoria (H), germinated spores (Sp), and

infected leaves at 2, 3, 4, 5, 6, and 7 days after infection. (B) Transient expression of the Sr33 and Sr50 coiled-coil (CC) domains with either YFP, *AvrSr50*, or HSP#18 in *N. tabacum* leaves. Image was taken 4 days after infiltration.

isolates identified transcript sequences only for the avirulence alleles (fig. S10), indicating that the virulence allele carrying the insertion sequence is not expressed.

We also examined *AvrSr50* diversity by means of amplification and sequencing from additional global *Pgt* races avirulent on *Sr50* (Fig. 2E and fig. S9). Two North American isolates (pathotypes MCCFC and DFBJ) were homozygous for the avirulence allele, whereas another (SCCL) was heterozygous, containing this allele and another, which encoded a protein differing from *AvrSr50* only by a single amino acid in the signal peptide region, with no effect on the predicted secretion. Thus, this latter is also likely to be an avirulence allele. This allele is also identical in sequence to the virulence allele in *Pgt632*, but without the insertion sequence, suggesting that it was the progenitor of this allele. An African isolate of the Ug99 group (TTKSK) contained a similar allele with one further conservative amino acid difference in the mature peptide, along with one copy of the insertion-disrupted virulence allele, and is thus heterozygous for *AvrSr50* avirulence. One isolate (race QCMJC) collected from the alternate sexual host barley and virulent on *Sr50* (7) contained one copy of the insertion-disrupted virulence allele along with another allele encoding a divergent protein with 12 amino acid differences from *AvrSr50*. We also extracted another allelic variant from published NGS data for North American isolate RKQQC (21), which encoded a protein with nine amino acid differences from *AvrSr50*. The RKQQC variant was recognized by Sr50 in *N. benthamiana* and in yeast, whereas the QCMJC variant was not

(Fig. 2, F and G, and fig. S11), which is consistent with the virulent phenotype of this isolate. The correlation between yeast protein interaction and induction of cell death in planta suggests that recognition specificity is mediated by direct interaction.

Analysis of the expression profiles of *Pgt* secreted protein genes in different infection stages detected eight distinct clusters (Fig. 3A, figs. S12 and S13, and table S7). *AvrSr50* is present in cluster number 8, which contains genes showing high relative expression in haustoria versus germinated spores and expression throughout infection. Cluster 4 shows a similar profile, but with smaller relative expression changes. Both clusters are overrepresented for genes encoding predicted nuclear localized effectors and genes specific to *Pgt* or *Puccinia* species (table S8). Thus, the genes in these expression clusters are likely to be enriched for effectors involved in host manipulation during infection. Many plant pathogenic fungi and oomycetes display a two-speed genome with rapidly evolving genes, such as those encoding effectors, located in repeat-rich regions (22). However, clusters 4 and 8 were not enriched for genes located close to repeat elements in the genome, which is consistent with the distribution of effector gene candidates in the *P. coronata* and *P. striiformis* genomes (23, 24). The *AvrSr50* protein shows nucleocytoplasmic distribution when expressed in *N. benthamiana* (fig. S14), and co-expression with the auto-active coiled-coil domains of Sr33 and Sr50 resulted in suppression of their cell-death signaling activity in tobacco (Fig. 3B). This suppression was also observed with several other HSP genes, including HSP#18

(Fig. 3B), and may reflect a function of these effectors in suppressing defense responses during infection of wheat.

The identification of *AvrSr50* here and *AvrSr35* by Salcedo *et al.* (25) will support resistance-gene deployment strategies because the *Avr* gene sequences can be used as molecular markers to survey the spatiotemporal distribution of these genes in *Pgt* populations and anticipate the evolution of virulence. For instance, heterozygosity for *AvrSr50* may predispose certain *Pgt* lineages to more rapid evolution of virulence toward *Sr50*. This information can help prioritize resistance genes for deployment in different geographic locations.

REFERENCES AND NOTES

1. P. G. Pardey *et al.*, *Science* **340**, 147–148 (2013).
2. R. P. Singh *et al.*, *Phytopathology* **105**, 872–884 (2015).
3. J. G. Ellis, E. S. Lagudah, W. Spielmeier, P. N. Dodds, *Front. Plant Sci.* **5**, 641 (2014).
4. P. N. Dodds, J. P. Rathjen, *Nat. Rev. Genet.* **11**, 539–548 (2010).
5. P. Olivera *et al.*, *Phytopathology* **105**, 917–928 (2015).
6. S. Periyannan, R. J. Milne, M. Figueroa, E. S. Lagudah, P. N. Dodds, *PLoS Pathog.* **13**, e1006380 (2017).
7. R. Mago *et al.*, *Nat. Plants* **1**, 15186 (2015).
8. K. J. Leonard, L. J. Szabo, *Mol. Plant Pathol.* **6**, 99–111 (2005).
9. N. M. Upadhyaya *et al.*, *Front. Plant Sci.* **5**, 759 (2015).
10. Materials and methods are available as supplementary materials.
11. C. Anderson *et al.*, *BMC Genomics* **17**, 667 (2016).
12. M. Ravensdale, A. Nemri, P. H. Thrall, J. G. Ellis, P. N. Dodds, *Mol. Plant Pathol.* **12**, 93–102 (2011).
13. L. J. Littlefield, M. C. Heath, *Ultrastructure of Rust Fungi* (Academic Press, 1979).
14. N. Luig, I. Watson, *Aust. J. Biol. Sci.* **25**, 335–342 (1972).
15. Y. Lei *et al.*, *Phytopathology* **107**, 329–344 (2017).
16. P. Williams, K. Mendgen, *Trans. Br. Mycol. Soc.* **64**, 23–28 (1975).

17. R. F. Park, *Aust. J. Agric. Res.* **58**, 558–566 (2007).
18. R. F. Park, J. J. Burdon, A. Jahoor, *Mycol. Res.* **103**, 715–723 (1999).
19. R. F. Park, C. R. Wellings, *Annu. Rev. Phytopathol.* **50**, 219–239 (2012).
20. W. S. Lee, K. E. Hammond-Kosack, K. Kanyuka, *Plant Physiol.* **160**, 582–590 (2012).
21. W. B. Rutter *et al.*, *BMC Genomics* **18**, 291 (2017).
22. S. Dong, S. Raffaele, S. Kamoun, *Curr. Opin. Genet. Dev.* **35**, 57–65 (2015).
23. M. E. Miller *et al.*, *bioRxiv* 179226 [Preprint]. 25 August 2017.
24. B. Schwessinger *et al.*, *bioRxiv* 192435 [Preprint]. 22 September 2017.
25. A. Salcedo *et al.*, *Science* **358**, 1604–1606 (2017).
26. M. Bernoux *et al.*, *Cell Host Microbe* **9**, 200–211 (2011).

ACKNOWLEDGMENTS

Work described here was supported by the TwoBlades foundation, the Grains Research and Development Corporation (grants US00067 and CSP00161), University of Minnesota Lieberman-Okinow and Stakman Endowments, Experimental Station USDA–National Institute of Food and Agriculture Hatch Funds (project MIN-22-058), and the Biotechnology and Biological Sciences Research Council (project BB/P016855/1). J.C. was supported by the Judith and David Coffey Life Lab and the Plant Breeding Institute, University of Sydney. J.G.E. has a scientific advisory role with the TwoBlades foundation. Sequence data was deposited in the National Center for Biotechnology Information Sequencing Read Archive under bioprojects PRJNA396463 and PRJNA415866. DNA of the rust isolates used in this study is available from R.F.P. under a

materials transfer agreement with the University of Sydney. We thank R. East and L. Ma for excellent technical assistance. Additional data are provided in the supplementary materials.

SUPPLEMENTARY MATERIALS

www.sciencemag.org/content/358/6370/1607/suppl/DC1
Materials and Methods
Figs. S1 to S14
Tables S1 to S9
References (27–48)
Data File S1

21 August 2017; accepted 3 November 2017
10.1126/science.aao4810

Loss of *AvrSr50* by somatic exchange in stem rust leads to virulence for *Sr50* resistance in wheat

Jiapeng Chen, Narayana M. Upadhyaya, Diana Ortiz, Jana Sperschneider, Feng Li, Clement Bouton, Susan Breen, Chongmei Dong, Bo Xu, Xiaoxiao Zhang, Rohit Mago, Kim Newell, Xiaodi Xia, Maud Bernoux, Jennifer M. Taylor, Brian Steffenson, Yue Jin, Peng Zhang, Kostya Kanyuka, Melania Figueroa, Jeffrey G. Ellis, Robert F. Park and Peter N. Dodds

Science **358** (6370), 1607-1610.
DOI: 10.1126/science.aao4810

Fungal effectors of wheat stem rust

The fungal pathogen Ug99 (named for its identification in Uganda in 1999) threatens wheat crops worldwide. Ug99 can kill entire fields of wheat and is undeterred by many of the disease-resistance genes that otherwise protect wheat crops. Two papers describe two peptides secreted by the fungus as it attacks the wheat (see the Perspective by Moscou and van Esse). Chen *et al.* show that fungal *AvrSr50* binds to the plant's immune receptor *Sr50*, and Salcedo *et al.* show that fungal *AvrSr35* binds to *Sr35*. Successful binding activates the plant's immune defenses. Removing or inactivating these *Avr* effectors leaves the plant defenseless and susceptible to disease.

Science, this issue p. 1607, p. 1604; see also p. 1541

ARTICLE TOOLS

<http://science.sciencemag.org/content/358/6370/1607>

SUPPLEMENTARY MATERIALS

<http://science.sciencemag.org/content/suppl/2017/12/20/358.6370.1607.DC1>

RELATED CONTENT

<http://science.sciencemag.org/content/sci/358/6370/1541.full>
<http://science.sciencemag.org/content/sci/358/6370/1604.full>

REFERENCES

This article cites 46 articles, 9 of which you can access for free
<http://science.sciencemag.org/content/358/6370/1607#BIBL>

PERMISSIONS

<http://www.sciencemag.org/help/reprints-and-permissions>

Use of this article is subject to the [Terms of Service](#)